3 Continuum Models of Multi-Walled Carbon Nanotubes

Abstract

Molecular mechanics simulations have been carried out to determine energetically favorable double-walled carbon nanotube (DWNT) structures, and analyze their infinitesimal extensional, torsional, radial expansion/contraction, and bending deformations. Loads are applied either to one wall or simultaneously to both walls of an open-ended DWNT. These results are compared against single-walled carbon nanotube (SWNT) results to determine differences and similarities between responses of SWNTs and DWNTs, and the validity of using SWNT results to predict the response of a MWNT. It is found that for small deformations such as simple tension and torsion, results for a DWNT can be derived from those for its constituent SWNTs within 3% error. Results of radial expansion/contraction of a SWNT are used to deduce an expression for van der Waals forces. Based on these results, a continuum model is proposed for a MWNT whose response to mechanical deformations is the same as that of the MWNT. The continuum structure is comprised of concentric cylindrical tubes interconnected by truss elements. Young's modulus, Poisson's ratio, the thickness of each concentric tube, and the stiffness of the truss elements are given. The proposed continuum model is validated by studying bending and the onset of global buckling deformations of a DWNT and its proposed equivalent continuum structure. Carbon nanotubes can be replaced by their equivalent continuum structures when deriving mechanical properties of nanotube reinforced polymeric composites.

3.1 Introduction

Although discovered first, multi-walled carbon nanotubes (MWNTs)[1] have not been studied as thoroughly as single-walled carbon nanotubes (SWNTs). This could partly be due to the higher specific stiffness and strength of a SWNT as compared to those a MWNT. However, in certain applications, MWNTs offer superior properties over SWNTs. For example, a MWNT is expected to have higher resistance to bending and buckling than a SWNT. Also, polymer matrix composites reinforced with MWNTs

probably have better dispersion characteristics than those reinforced with SWNTs. MWNTs do not have the same propensity to clump as SWNTs and may disperse more easily. MWNTs are easier to manufacture and are therefore less expensive than SWNTs. They could conceivably be used as a bearing[2] and as a pipe to transport fluids[3].

Much of the literature on the determination of elastic moduli of SWNTs is summarized in Sears and Batra[4], and is not reported here. The reader is also referred to the review paper of Qian et al.[5] for a summary of earlier works.

When loaded in tension, a MWNT is likely to have a lower specific stiffness than a SWNT because only the outermost wall of a MWNT supports the load. Atoms on adjacent walls of a MWNT do not share molecular bonds; therefore, interactions between them are only through van der Waals forces. Schonenberger et al.[6] have demonstrated the possibility of sliding inner-walls of a MWNT in a telescopic-like motion; this is attributed to the low energy barriers for sliding the inner-walls. Yu et al.[7] found during tensile tests that the tensile strength is at least an order of magnitude lower than what it would be if the axial stress was uniformly distributed over all layers of a MWNT. They found that the outer tube ruptured at the tensile limit stress/strain, and then slid over the inner tube. Yu et al.[8] studied the sliding between nested shells of MWNTs and observed both stick-slip and smooth pullout motions. The inner walls can resist lateral or inward radial deflections of the outer wall since they affect van der Waals forces. Thus, an inner wall will resist the radial contraction of an outer wall in tensile deformations of a MWNT. In compressive deformations, an inner wall will begin to carry loads at some point due to the reduction in the distance between the end-caps and the consequent increase in van der Waals forces; when this occurs depends on the geometry of the end-cap. Two end-cap geometries are shown in Figure 3.1 that is taken from Qian et al.[5]; it is clear that there is a wide variation in the distance between end-caps of two adjacent walls. Thus the specific Young's modulus of a MWNT is likely to be lower than that of a SWNT in tension.

Treacy et al.[9] have experimentally studied flexural vibrations of a cantilever MWNT, and Yu et al.[7] have performed tensile tests on a MWNT by applying loads only to its outermost wall. Treacy et al. found that Young's modulus E varied from 0.40 to 4.15 TPa with an average value of 1.8 TPa, while Yu et al. obtained values in the range of 0.27 to

0.95 TPa. Salvetat et al.[10] and Wong et al.[11] also performed bending tests using an atomic force microscope and found, respectively, 0.81 ± 0.41 and 1.28 ± 0.59 TPa for Young's modulus. These values are comparable to those obtained from molecular mechanics (MM) simulations on a SWNT. Lourie and Wagner[12] used Raman spectroscopy to determine the modulus of MWNTs embedded in a matrix as fibrous reinforcements, and obtained Young's modulus ranging from 1.7 to 2.4 TPa.

The deduction of material moduli from test results (and also from results of MM/molecular dynamics (MD) simulations) requires the consideration of a continuum structure equivalent in mechanical response to the MWNT tested. Many studies[7, 9-11]

have assumed that the response of a MWNT is equivalent to that of a linear elastic isotropic homogeneous cylindrical tube of outer radius equal to that of the outermost wall of the MWNT and wall thickness 3.4N Å, where 3.4 Å and N equal, respectively, the mean distance between two adjacent walls and the number of walls in the MWNT. We note that the imposed mechanism to model the van der Waals forces is a rigid connection.

Based on potentials for bond deformations and van der Waals forces, Li and Chou[13] studied deformations of a double-walled carbon nanotube (DWNT) by interconnecting atoms with trusses and finding their stiffnesses from bond potentials. They analyzed tensile and torsional deformations, and computed Young's modulus values ranging from 0.95 to 1.15 TPa, and the shear modulus values between 0.38 and 0.46 TPa. When only the outer wall was loaded, they found a little to no transfer of load to the inner wall due to van der Waals forces.

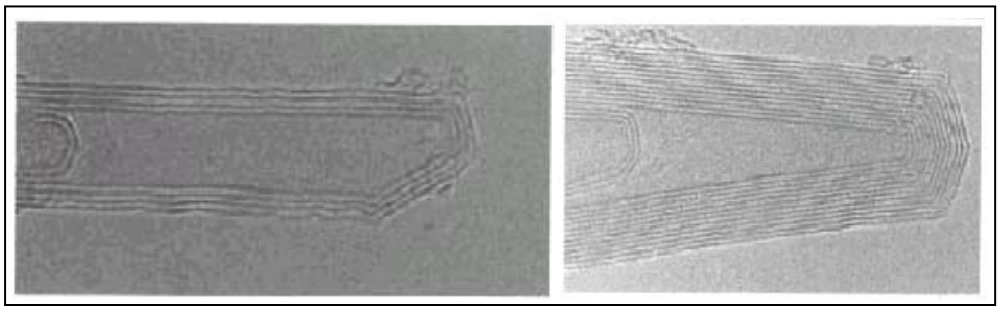

Figure 3.1. TEM image of the end-cap geometry of MWNTs (From Qian et al.[5])

Table 3.1. Literature values of Young's modulus for a MWNT; these studies assumed that a MWNT can be modeled as a linear elastic, homogeneous and isotropic cylindrical tube as described above.

Investigation	Year	avg. Modulus (TPa)	Method	Test
Treacy et al. (Ref. 6)	1996	1.8	experiment	thermal vibrations
Wong et al. (Ref. 8)	1997	1.28	experiment	cantilever bending
Lourie & Wagner (Ref. 9)	1998	2.8-3.6	experiment	Raman spectroscopy
Salvetat et al. (Ref. 7)	1999	1.28	experiment	3 point bending
Yu et al. (Ref. 4)	2000	0.27-0.95	experiment	tension
Li and Chou (Ref. 10)	2003	0.95-1.15	FEA	tension

Salvetat et al. found that MWNTs grown by the arc discharge method have Young's modulus of 1TPa, and Young's modulus of those grown by the catalytic decomposition of hydrocarbons is one to two orders of magnitude lower. Thus only highly ordered and well-graphitized MWNTs having strong carbon-carbon bonds within each layer and have Young's modulus comparable to that of graphite. MWNTs grown by the catalytic decomposition technique have more defects than those formed by the arc discharge method.

Ru[14] used a continuum approach to study the effect of van der Waals forces on the buckling response of a DWNT, modeled tube walls as cylindrical shells with a bending stiffness, $D(t)=Et^3/(12(1-\nu^2))$, where t is the wall thickness of the equivalent cylindrical shell and ν Poisson's ratio, and assumed that shell walls interact through pressure, p, given by, $p_iR_i = p_oR_o$, where R is the wall radius and subscripts i and o signify, respectively, the inner and the outer wall of the DWNT or the cylindrical shell. Ru's analysis predicts that the critical strain for shell wall buckling of a DWNT is lower than that of a SWNT. He assumed that the pressure, p, is proportional to the distance between the two adjacent walls, or the gap between the walls, and did not find the value of the constant of proportionality that will give reasonable values of van der Waals forces. Galanov et al. (2002) considered two models of a MWNT; in one they replaced each inner wall by a membrane and in the second a MWNT by a cylindrical tube.

Based on MM simulations of a SWNT deformed in tension/compression and torsion, and the relation $E = 2G(1+\nu)$ valid for linear elastic isotropic materials, Sears and Batra[4] found that the response of an isotropic, homogeneous and linear elastic cylindrical tube with Young's modulus E = 2.52 TPa, shear modulus G = 0.96 TPa, and wall thickness t =

1.34 Å to mechanical deformations is equivalent to that of the SWNT. These values were found to be nearly the same for SWNTs of various diameters and helicities. Average values of material and geometric parameters for the (8,0), (12,6), (16,0), (25,0), (48,0) and (10,10) tubes are E = 2.46 TPa, G = 0.99 TPa, Poisson's ratio ν = 0.21 and t = 1.35 Å with coefficients of deviation of 0.04, 0.03, 0.05 and 0.01 respectively. Liew et al.[15] found that the classical shell theory with the wall thickness of 1.54 Å gave results in close agreement with their predictions of the buckling load from the MD simulations. Pantano et al.[16] modeled a DWNT as two concentric thin cylindrical shells each having t = 0.75 Å, ν = 0.19, E = 4.84 TPa, and analyzed its buckling deformations by the finite element method. The van der Waals force was simulated as equal and opposite pressures on the outer wall of the inner cylinder and the inner wall of the outer cylinder with the pressure varying affinely with the distance between the two walls. The shell walls were assumed to be initially stressed due to their curvatures with the magnitude of the stress varying inversely as the radius of the shell wall.

Whereas for a SWNT the equivalent continuum structure can be either a solid fiber or a cylindrical tube, for a MWNT the equivalent continuum body can be one of the following three: a solid fiber, a cylindrical tube, and a structure comprised of multiple concentric cylindrical tubes. There is no easy way to account for van der Waals forces in the first two continuum structures even though, as mentioned above, the second one has often been used. Accordingly, we propose that the continuum structure equivalent in mechanical response to a MWNT be comprised of concentric cylindrical tubes with the number of tubes equal to the number of walls in a MWNT. The next tasks are to find the mean diameter and the thickness of each continuum tube, a way to interconnect concentric tubes in order to model the action of van der Waals forces between adjacent walls of a MWNT, and values of elastic constants for the material of each concentric tube. In an attempt to elucidate upon the interaction between two adjacent walls of a MWNT due to van der Waals forces, we seek answers to the following four questions for a DWNT by using MM simulations with the MM3 potential: (i) Does the inner wall slide freely in the outer wall as is commonly assumed? (ii) Can a simple superposition of solutions for SWNTs be used to obtain the response of a MWNT? (iii) What are quantifiable differences between responses of a SWNT and a DWNT to commonly

studied simple deformations such as axial tension/compression, torsion and bending? (iv) What is more important in the construction of MWNT structures, relative helical angles or wall separation distance?

We perform a series of MM simulation tests on several DWNTs. These tests are similar to those performed on a continuum structure in the Mechanics of Materials Laboratory. The MM simulations of infinitesimal axial and torsional deformations reveal that the response of a DWNT is similar to that of a SWNT. We then study radial expansion/contraction of a DWNT to find an expression for the van der Waals force between atoms on two adjacent walls. All of this information is synthesized to propose a continuum structure of a MWNT whose response to infinitesimal mechanical deformations is equal to that of the MWNT. Many anticipated engineering applications of MWNTs will involve infinitesimal deformations. In order to establish the validity of the proposed continuum model, the response in bending and global buckling of the axially compressed continuum structure is compared with that of MM simulations on the corresponding DWNT.

Contributions of this work include the following: (i) Determination of relaxed configurations of DWNTs prior to simulating their deformations. This is equivalent to annealing a continuum structure prior to testing it. Whereas annealing of a continuum structure usually relieves all prior internal stresses, there is no guarantee that a DWNT in a relaxed configuration is free of all internal stresses. It, however, provides the same base configuration for all DWNTs simulated herein. (ii) Proposal of a continuum structure energetically equivalent in mechanical response to a MWNT in the sense that for the same average axial or shear/torsional strain, the continuum and the atomic structures have the same energies of deformation. The continuum structure is comprised of initially stress-free concentric cylindrical tubes interconnected by truss elements. (iv) Validation of the continuum model by comparing predictions from it with those from the MM simulations. The approach is valid for any MM potential. It uses values of the strain energy of deformation and strains averaged over the specimen. It does not use the Cauchy-Born rule.

A limitation of this work is that it is valid for infinitesimal deformations of an atomically perfect MWNT; thus fractures are not considered. Atomic studies on fracture

of CNTs[17] have given fracture strains under axial tensile deformations of ~10%. Thus the limitation of the present work is not as severe as it first appears. However, it is not applicable to problems involving folding and unfolding of tubes where large elastic strains are induced. Its extension to finite deformations is nontrivial since a constitutive relation for a second-order isotropic elastic material has six material constants whose evaluation will require many more types of tests than the simple tension/compression and torsion. An alternative is to adopt the approach of Arroyo and Belytschko[18] or that of Zhang et al.[19]. Arroyo and Belytschko developed a finite element model for MWNTs. Rather than using a thin shell theory, they replaced a tube wall by a membrane made of a hyperelastic material and deduced its mechanical properties directly from the Tersoff-Brenner potential, crystal elasticity and a modified Cauchy-Born rule. The pressure equivalent to that exerted by the van der Waals forces was applied to the membrane. For torsional, bending and compressive deformations, they successfully reproduced local buckling, kinking, and rippling effects, which were very close to the shapes obtained by the MM simulations.

The rest of the paper is organized as follows. Details of the molecular mechanics (MM) simulations are given in Section 2 where various relaxed configurations of DWNTs are also described. Section 3 gives MM simulations results for simple deformations of a DWNT and also gives an expression for the van der Waals force. The equivalent continuum structure is deduced in Section 4, and is validated in Section 5 by comparing results of bending and global buckling deformations on the continuum structure and the corresponding DWNT. Conclusions of this work are summarized in Section 6.

3.2 Molecular Mechanics Simulations

3.2.1 Molecular Mechanics Potential

The MM3 class II pair-wise potential with both higher-order expansions and cross-terms and type 2 (alkene) carbon atoms[20] is used. This potential has both higher-order expansions and cross-terms and is appropriate for carbon nanotubes due to the similarity between graphitic bonds in the nanotube and the aromatic protein structures for which the

potential was constructed. Numerous MM potentials and quantum theories have been used to predict a wide range of mechanical responses of nanotubes. Of these MM potentials, the MM3 potential yields results for SWNTs that are close to those found experimentally.

The MM3 potential is described by Eq. (1) in which the terms U_s, U_θ and U_ϕ are the primary bond deformation terms; the term, U_{VdW}, is the non-bonded van der Waals term, and $U_{s\phi}$, $U_{\phi s}$ and $U_{\theta\theta'}$ represent cross interactions between the variables. Parameters r, θ and ϕ used in the equation are shown in Figure 3.2. A subscript, 0, on a variable signifies its value in the unstressed equilibrium configuration. The total energy of a body equals the sum of the potential for all atoms in the body (the index j in Eq. (3.1) ranges over bonded atoms, and the index k over all atoms).

$$
\begin{aligned}
U_s &= 71.94K_s(r-r_0)^2[1-2.55(r-r_0)+(\tfrac{7}{12})2.55(r-r_0)^2] \\
U_\theta &= 0.02191K_\theta(\theta-\theta_0)^2 \times \\
&\qquad [1-(\theta-\theta_0)+5.6(10^{-5})(\theta-\theta_0)^2-7.0(10^{-7})(\theta-\theta_0)^3+9.0(10^{-10})(\theta-\theta_0)^4] \\
U_\phi &= (V_1/2)(1+\cos\phi)+(V_2/2)(1-\cos 2\phi)+(V_3/2)(1+\cos 3\phi) \\
U_{VdW} &= \varepsilon\{-2.25(r_v/r)^6+1.84(10^5)\exp[-12.00(r/r_v)]\} \\
U_{sb} &= 2.511K_{sb}[(r-r_o)+(r'-r'_0)](\theta-\theta_0) \\
U_{s\theta s} &= 11.995(K_{\phi s}/2)(r-r_0)(1+\cos 3\phi) \\
U_{\theta\theta'} &= -0.021914K_{\theta\theta'}(\theta-\theta_0)(\theta'-\theta'_0)
\end{aligned}
\tag{3.1}
$$

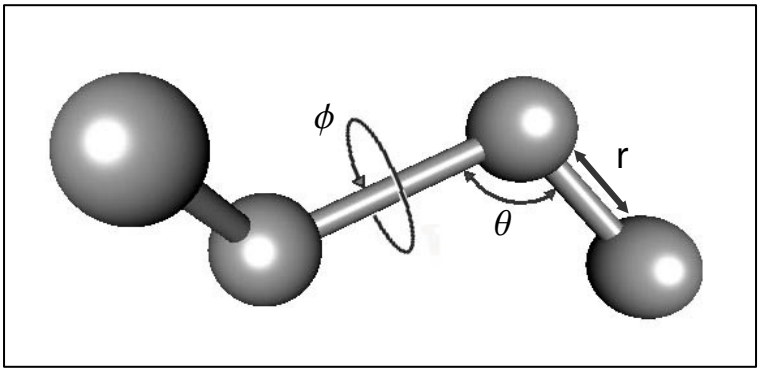

Figure 3.2. Definitions of variables r, θ and ϕ used in defining pair-wise MM3 potentials.

Values of constants K_s, K_θ, V_1, V_2, V_3, ε_0, r_v, K_{sb}, $K_{\phi s}$ and $K'_{\theta\theta}$ are given in Zhou et al. (2000). Note that the van der Waals force between two atoms varies as $(r_v/r)^{-6}$ and $exp(-12r/r_v)$ which is quite different from that in the Lennard-Jones potential.

For four MM potentials, namely the MM3, the Amber, the Morse and the TB, the bond strain energy, U_s, versus the bond strain is plotted in Figure 2.2. For bond strains of about 5% the curves for these potentials are nearly coincident. For simple tensile deformations of a SWNT simulated with the MM3 potential (Figure 2.7) the potential energy due to bond stretching essentially equals the total energy of the SWNT as contributions from other terms cancel with each other. However, for simple axial compressive deformations, the bond stretching, the angle bend and the van der Waals terms make nearly equal contributions to the total energy of deformations. Also, at the onset of global buckling, the total energy of the SWNT abruptly decreases.

The Tersoff-Brenner potential has been used by Zhang et al.[19] to build an equivalent continuum structure. Sears and Batra[4] have compared predictions from it with those derived from the MM3 potential. An advantage of MM3 potential is that it is applicable to a wider class of hydrocarbons and can also be employed to study the interaction between MWNTs and the surrounding polymeric matrix.

3.2.2 Computer code

We used the computer code TINKER[21] to analyze mechanical deformations of MWNTs. The potential energy of the structure is minimized through an adaptive minimization routine which utilizes either a truncated Newton or a negative curvature technique. Except where noted, all simulations used a non-bonded cutoff value of 30 Å, and minimized the potential energy to within 0.001 kcal/mol/ Å rms.

3.2.3 MWNT structures

Before a MWNT may be tested a relaxed configuration (i.e. the one of minimum potential energy under no external loads) should be determined to establish a ground state for its potential energy. The nanotube atomic structures are closed structures constructed of whole hexagonal rings which dictate that they must be discrete in size and structure. The White et al.[22] notation for classifying SWNTs by their (a,b) wrapping vector

describes each structure uniquely. This classification system is extended to incorporate MWNTs into the ((a,b),(c,d),…) notation where (a,b) describes the innermost SWNT. Thus numerous distinct MWNT structures are available; many of these were examined to determine which were energetically more favorable. The ideal wall separation distance for MWNTs has been found to be ~3.4 Å.

Thus only SWNTs with estimated separation distances between 3.3 to 3.5 Å were used to construct a range of DWNTs, and all other DWNTs were assumed to be energetically unfavorable due to the much higher inter wall van der Waals energies. For a particular outer wall, several inner wall structures can meet this criterion. Thus, effects of helicity and wall separation distance may be ascertained to find out whether one or both or none plays a more important role in determining MWNT structures.

The MWNT configurations were constructed by placing one relaxed SWNT on the outside of another relaxed SWNT and repeated for as many walls as desired. The procedure for determining the relaxed configuration of a SWNT can be found in Sears and Batra[4]. In summary it involves estimating the SWNT configuration and then minimizing the potential energy of the structure. The DWNT walls were trimmed to coincident lengths of 200 Å. The strain energy of a MWNT was minimized to convergence value of 0.001 rms. This process invariably deforms MWNT walls from their relaxed SWNT configurations. The van der Waals forces typically cause radial deformations of the walls as they try to move the walls towards the ideal wall separation distance. This process will also cause axial deformations due to the Poisson effect. Furthermore, the MWNT walls will tend to shift axially so that their end faces are no longer coincident. For example, the ((a,0),(b,0)) type DWNTs were found to shift so that the hexagonal rings took up a staggered configuration rather than a stacked configuration. These open ended nanotubes were preferred to periodic nanotubes because the latter can not guarantee that walls are under the same strain. Also, only one wall can not be deformed in a periodic nanotube, which negates tests to determine whether or not two adjacent walls of a MWNT can deform independently of each other. Various DWNT relaxed configurations are listed in Table 2 where the separation strain, $\varepsilon_{s,}$ is defined as $(s_r - s_a)/ s_a$; s_r and s_a equal, respectively, the distance between walls of the relaxed

configurations of the two SWNTs, and the distance between them in the relaxed configuration of the resulting DWNT.

Table 2 has been formatted to show different inner walls of a DWNT with the structure of the outer wall fixed. For example, for the ((a,b),(20,8)) DWNT series, the (11,7) inner tube yields the lowest separation deformation. The lowest separation strains occurred for DWNTs for which the distance between the walls of the relaxed configurations of the two constituent SWNTs was about 3.43 Å, which equals the ideal distance between the two adjacent walls. It was expected that the separation strain would occur in a balanced manner, that is, the inner wall would move outwards and the outer one inwards. However, while this occurred in most cases, both walls contracted in other cases. Intriguingly, for the three DWNTs which experienced the least separation strain, both walls contracted. It was also expected that tubes with the lowest separation strains would have the lowest intermolecular energy. Of the five series of DWNTs shown in the Table, this was found to be true. The data listed in Table 3.2 is plotted in Figure 3.3 to clearly evince the following two trends. The intermolecular energy exhibits a parabolic shape around the ideal wall separation strain, and the separation strain varies almost linearly with the distance between the walls of the relaxed configurations of the DWNT. No significant correlations were found between the intermolecular energy and the helicities of the DWNTs. However, the preference for staggered rather than stacked rings for the ((a,0),(b,0)) tubes shows that the tube's structure does have an effect, however, it is less significant than the effect of the separation distance.

3.2.4 Virtual Experiments

The minimum energy configuration for the molecular structure is first found. That is, all atoms are allowed to move freely until the total energy of the structure reaches a minimum. This minimum energy configuration of the structure is henceforth referred to as the relaxed structure. All simulations are displacement controlled, i.e., appropriate displacements are prescribed on atoms near the end faces of the tube. Also, all MWNTs considered are open-ended; thus the effect of end caps is not modeled. The open ends locally change the bonding character of the structure and may result in edge effects. In order to mitigate these, boundary conditions were applied to atoms ~ 1 diameter away

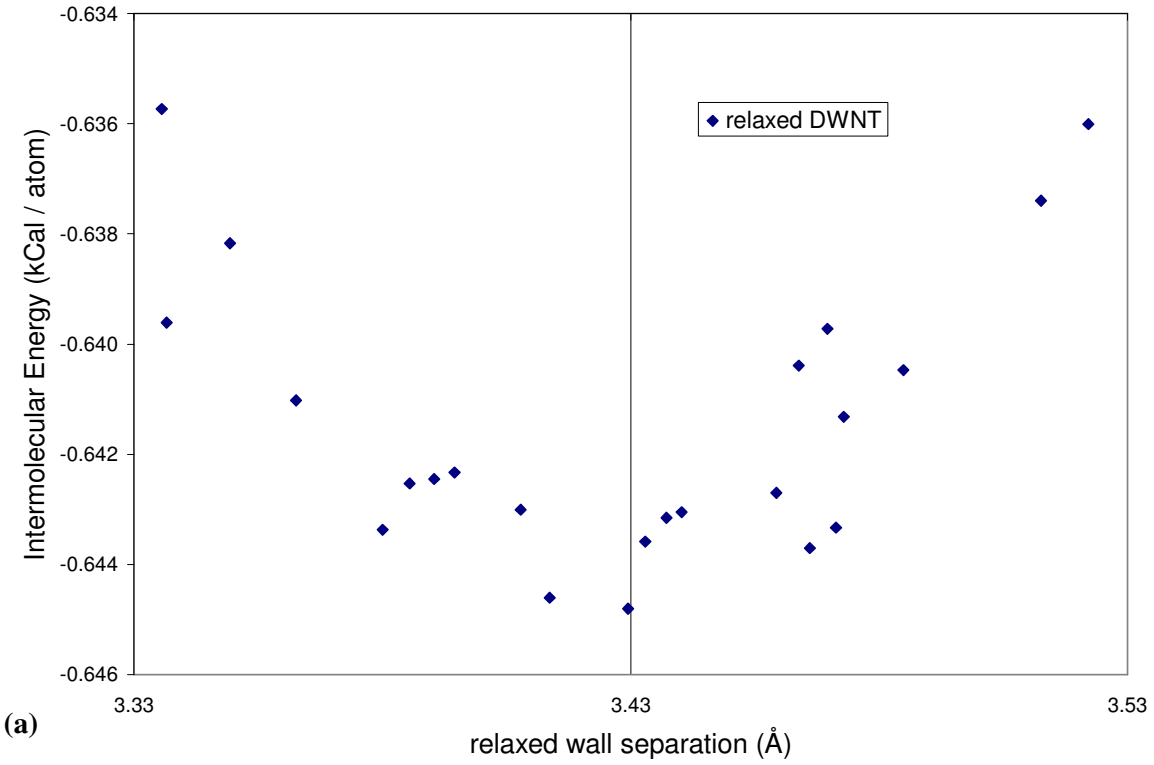

(a)

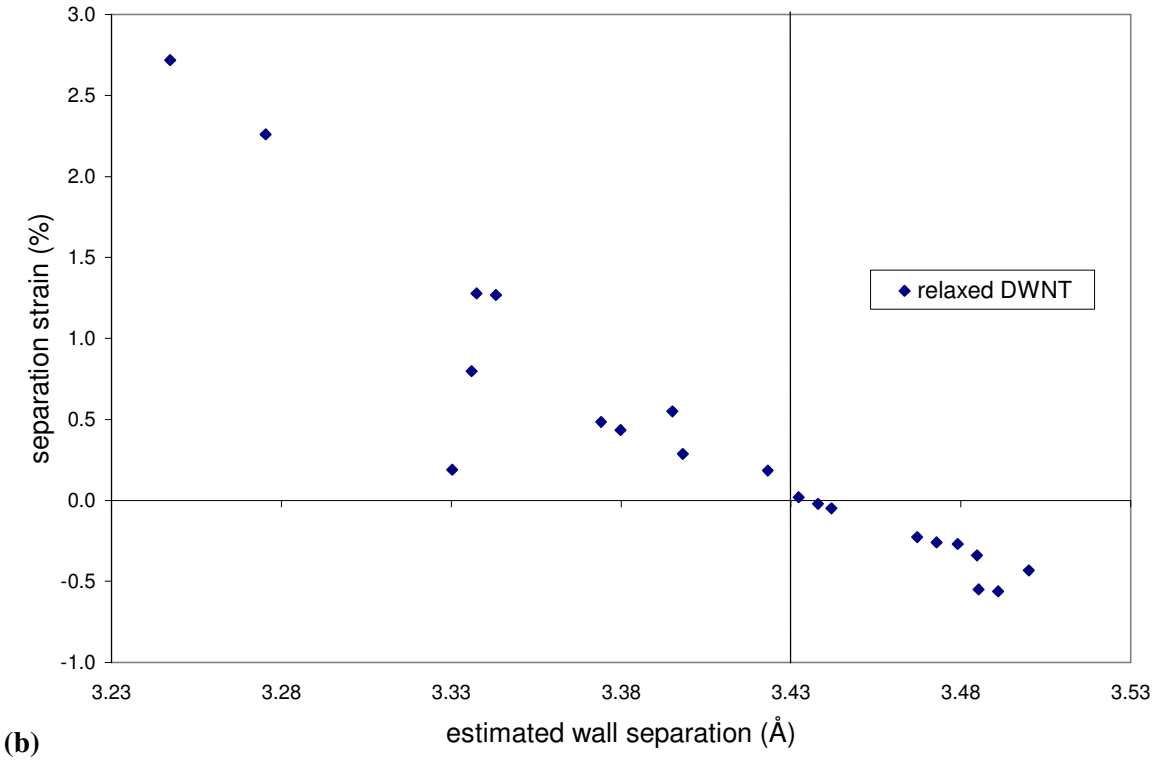

(b)

Figure 3.3. For DWNTs, (a) intermolecular energy vs. wall separation distance, and (b) the separation strain vs. the initial distance between walls of relaxed SWNTs constituting the DWNT.

from the end faces and tube's aspect ratio (length/diameter) was kept above ten. Local effects, such as necking or swelling during axial deformation, occur within 2 Å of the atoms where boundary conditions were applied; these were found to have negligible effect on the total energy of the system. With atoms where displacements are specified kept fixed, remaining atoms are allowed to move freely till the potential energy of the system is minimized. The difference between the potential energies of the deformed and the relaxed configurations of the tube gives the energy required to deform it. Numerical experiments showed that the precise value of the distance from the free ends of atoms where displacements are enforced did not affect results.

In a laboratory set-up, loads can only be applied to the outer walls of a DWNT and are transferred to the inner wall through non-bonded interactions among atoms on the two walls. Accordingly, in one of the simulations mimicking either simple tensile or simple torsional deformations, boundary conditions were applied only to atoms on the outer wall. These simulations are termed the "slip" cases since no external loads are applied to the inner walls. In the second set of simulations, termed "fully constrained", the loads in terms of displacement boundary conditions are applied simultaneously to both walls of a DWNT. In an axial compression test performed on a MWNT in a laboratory, the capped ends will transfer the load from the outer to the inner wall. Our fully constrained simulations correspond to the assumption that the load transferred instantaneously and both walls are strained equally.

Periodic boundary conditions to simulate an infinitely long DWNT could not be enforced at the end faces of a DWNT of finite length because of the offset and differences in lengths between its two walls in the relaxed configuration.

Table 3.2. Summary of tube structures, deformations from SWNT relaxed configurations, and non-bonded, inter wall energy comparisons. The lowest separation strain for each series is shown in bold. Furthermore, ε_{ri} = circumferential strain in the inner wall, ε_{ro} = circumferential strain in the outer wall, E_{int} = inter atomic energy, circumferential strain = radial displacement / initial radius.

inner wall	outer wall	s_r (Å)	s_a (Å)	ε_s (%)	ε_{ri} (%)	ε_{ro} (%)	E_{int} (kCal/atom)
9,9	20,8	3.470	3.479	-0.269	0.006	-0.097	-0.6397
10,8	20,8	3.459	3.467	-0.226	-0.011	-0.091	-0.6427
11,7	20,8	3.433	3.432	**0.020**	-0.066	-0.034	**-0.6436**
12,6	20,8	3.390	3.374	0.483	-0.168	0.069	-0.6424
16,0	20,8	3.337	3.330	0.188	-0.007	0.063	-0.6396
9,9	25,0	3.473	3.485	-0.338	0.017	-0.116	-0.6413
10,8	25,0	3.464	3.473	-0.259	-0.003	-0.099	-0.6404
11,7	25,0	3.437	3.438	**-0.021**	-0.057	-0.044	**-0.6432**
12,6	25,0	3.395	3.380	0.435	-0.158	0.058	-0.6423
16,0	25,0	3.363	3.336	0.796	-0.233	0.137	-0.6410
9,9	16,13	3.522	3.547	-0.696	0.105	-0.200	-0.6360
10,8	16,13	3.513	3.535	-0.632	0.087	-0.185	-0.6374
11,7	16,13	3.485	3.500	-0.433	0.040	-0.137	-0.6405
12,6	16,13	3.440	3.442	**-0.049**	-0.050	-0.049	**-0.6431**
16,0	16,13	3.408	3.398	0.286	-0.123	0.026	-0.6430
20,8	34,0	3.386	3.343	**1.267**	-0.248	0.153	-0.6425
25,0	34,0	3.380	3.337	1.278	-0.246	0.157	**-0.6434**
16,13	34,0	3.349	3.275	2.258	-0.388	0.300	-0.6382
21,7	34,0	3.336	3.247	2.718	-0.453	0.364	-0.6357
20,8	26,13	3.471	3.491	-0.562	0.035	-0.128	-0.64333
25,0	26,13	3.466	3.485	-0.550	0.036	-0.124	-0.6437
16,13	26,13	3.429	3.423	**0.185**	-0.077	-0.007	**-0.6448**
21,7	26,13	3.414	3.395	0.549	-0.135	0.047	-0.6446

3.3 Response to Simple Deformations

3.3.1 Axial Deformations

We first investigate if the strain energy of deformations of a DWNT under applied axial tractions or axial displacements equals the sum of the strain energies of the constituent tubes subjected to the same boundary conditions as the DWNT. Such a comparison will also illuminate the effect, if any, the van der Walls force has on deformations of a DWNT. Results for several DWNTs are shown in Figures 3.4 and 3.5. To properly compare results for different nanotubes, the strain energy per atom is used as a metric and plotted against the axial strain. The buckling of a tube in axial compression is signified

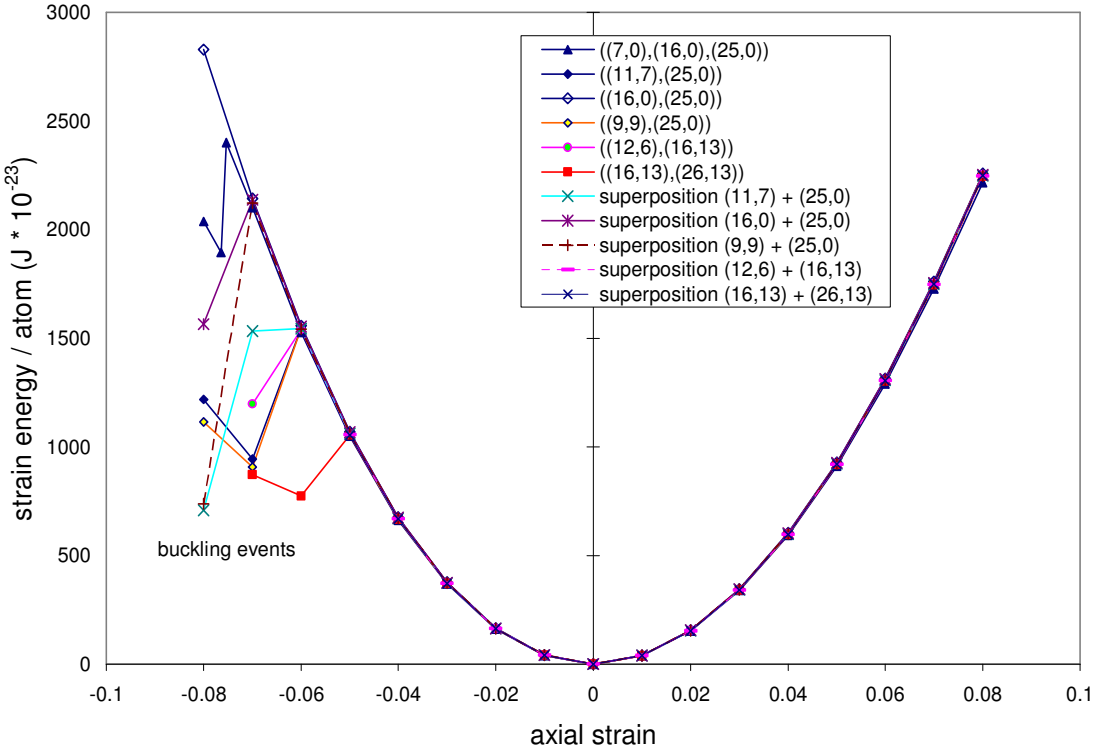

Figure 3.4. For axial deformations, strain energy of a fully constrained DWNT vs. axial strain, and sum of strain energies of the constituent SWNTs vs. axial strain.

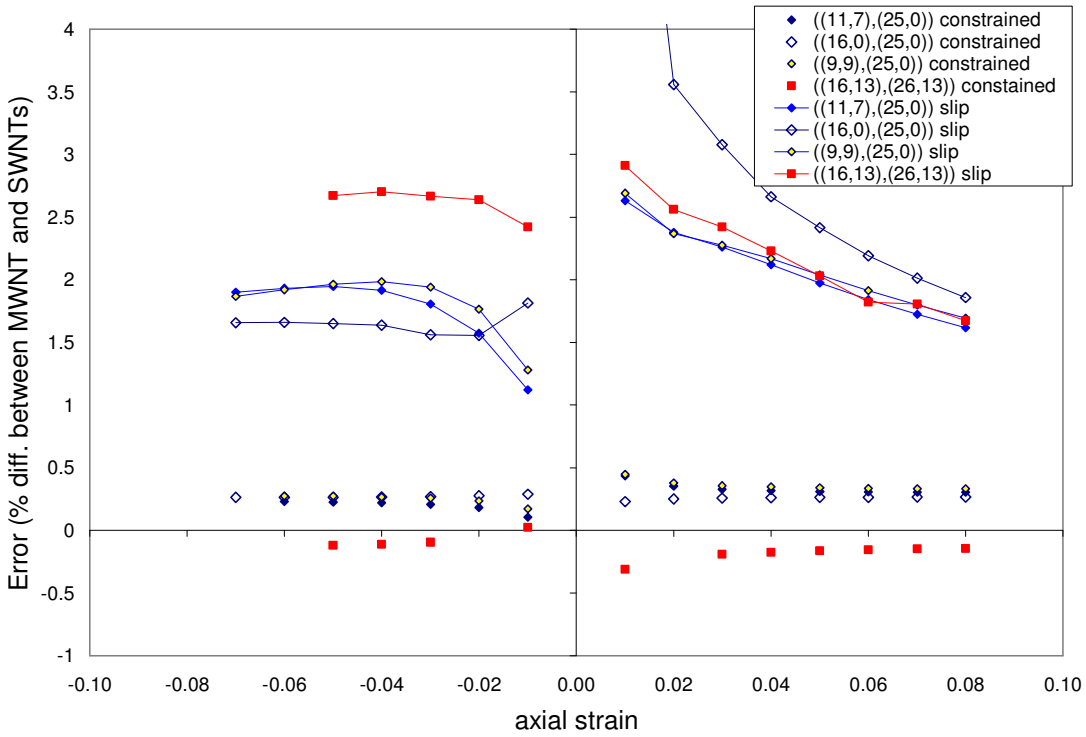

Figure 3.5. Differences in strain energy/atom of a DWNT and the sum of strain energies/atom of constituent SWNTs for both fully constrained (unconnected points), and slip (solid curves) cases.

by the sudden drop in the strain energy of deformation with an increase in the axial compressive strain. Prior to buckling, for a given value of the axial strain the strain energy per atom is very nearly the same for the DWNTs and the TWNT (triple-walled nanotube); it differs from the sum of the strain energies per atom of the constituent SWNTs by less than 0.5% for the fully constrained cases and by less than 3.5% for the slip cases. The rather larger difference for the slip cases is most likely caused by the van der Waals forces. In the fully constrained case, both walls are strained axially by the same amount and will also deform radially nearly the same amount due to Poisson's effects. Thus the wall separation remains nearly the same and no significant change in van der Waals forces will accrue. However, in the slip case, the inner wall will not deform radially due to Poisson's effects but the outer wall will deform radially, the wall separation will change and some energy of deformations due to the change in van der Waals force will accrue. This is supported by the plots included in Figure 3.6 of the strain energy/atom due to the van der Walls force and the difference in the strain energies/atom of a DWNT with only the outer wall constrained and the strain energy/atom of its constituent outer SWNT. Note that the two quantities are close to each other.

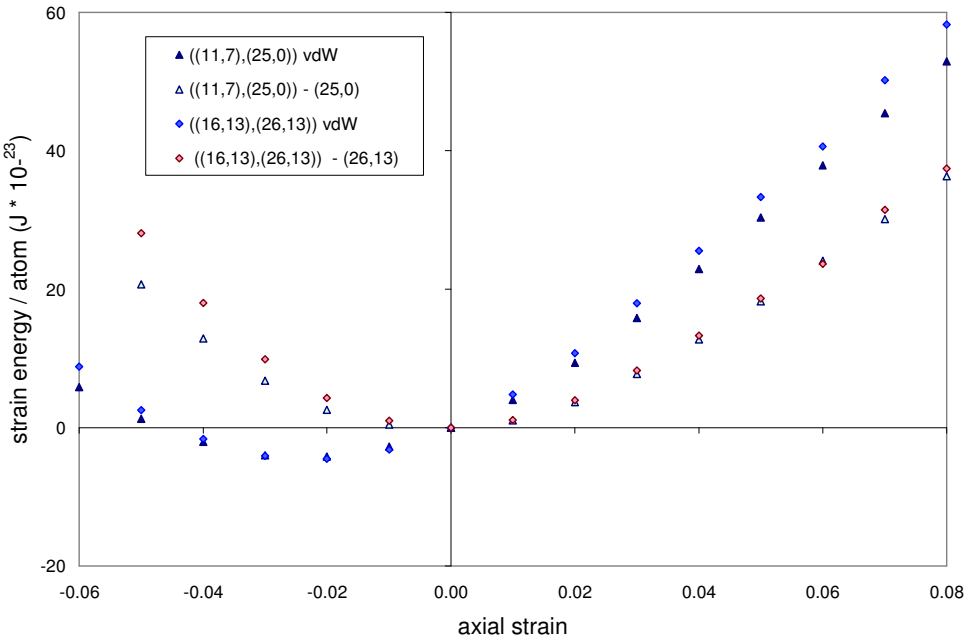

Figure 3.6. Comparison of strain energy due to intermolecular van der Waals forces and the difference in strain energies of a DWNT loaded under slip conditions and identically loaded constituent SWNT.

These results imply that the response of a DWNT is independent of the helicity. Furthermore, the strain energy of axial deformations due to van der Walls forces is about 3% of the total strain energy. Thus, the error involved in using results of axial deformations, prior to the onset of either local or global buckling, of SWNTs to predict those for a MWNT is approximately 3%.

3.3.2 Torsional Deformations

The torsional test was simulated in the same way as the simple tension test, i.e., circumferential displacements of atoms corresponding to the desired angle of twist were determined and applied to atoms ~ one diameter from the free ends. With atoms where displacements are prescribed kept fixed, other atoms were allowed to move freely till the potential energy of the system was minimized. The strain energy/atom for infinitesimal torsional deformations of the inner SWNT of a DWNT with no loads applied on the outer wall (slip condition), for various wall structures, is presented in Figure 3.7, and for those when both tubes are twisted simultaneously through the same angle (fully constrained case) in Figure 3.8. The angle of twist per unit tube length is used as a metric because for the same angle of twist/length the shear strains of different walls vary due to their different radii. The deviations from the parabolic energy response at higher angles of twist/length are most likely due to the buckling of tubes. As for the axial deformations, the strain energy for infinitesimal torsional deformations of a DWNT equals the sum of the strain energies of torsional deformations of the constituent SWNTs, and the maximum difference between the two values is ~ 1%.

Thus the effects of helicities and the van der Walls force between adjacent walls of a DWNT on its torsional deformations are negligible.

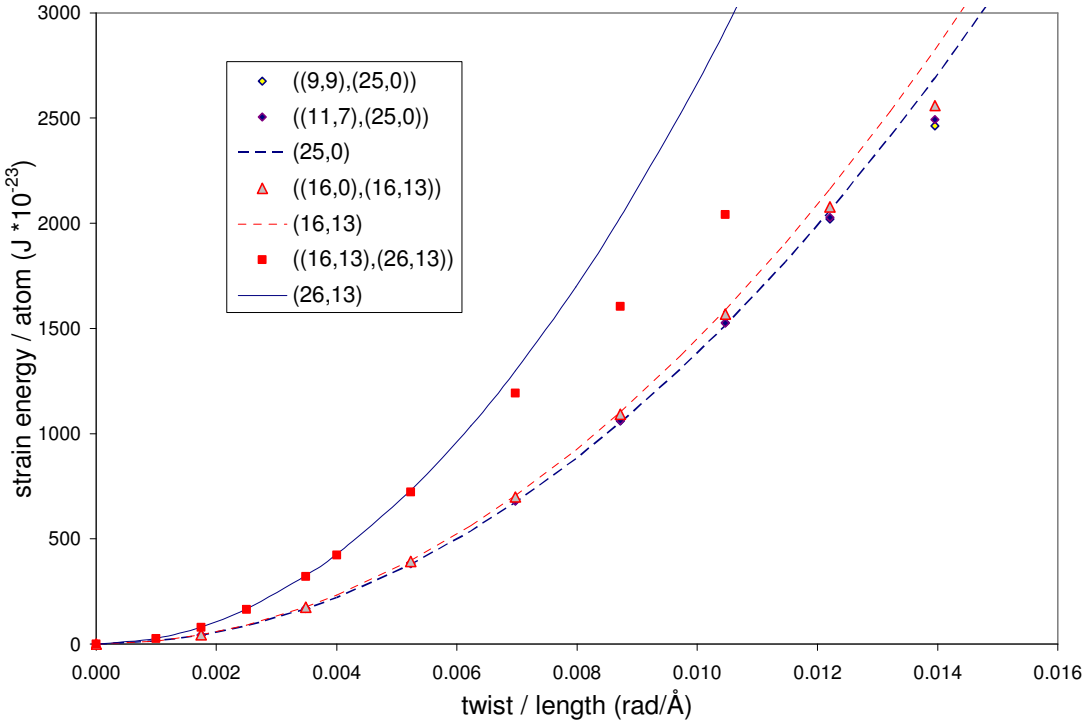

Figure 3.7. Strain energy/atom for torsional deformations with loads applied only on the outer wall of DWNTs (slip condition), and SWNTs with the same atomic structures as those of the outer walls of DWNTs.

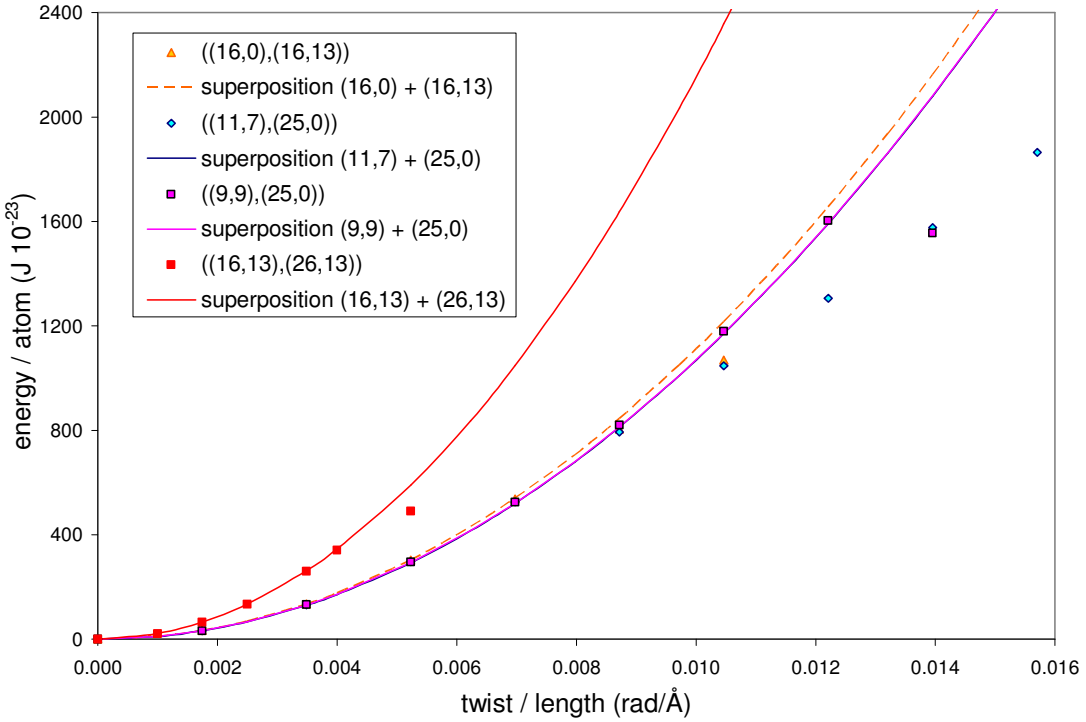

Figure 3.8. Strain energy/atom for torsional deformations of fully constrained DWNTs and that obtained by adding the strain energy/atom of their constituent SWNTs.

3.3.2a Buckling under torsional loads

One situation where the response of a MWNT differs from that of its constituent SWNTs is buckling. A nanotube (either SWNT or MWNT) was assumed to have buckled when either the strain energy of deformations dropped significantly for an infinitesimal increase in the load or lateral deflections were very large. These invariably corresponded to a noticeable increase in the number of iterations needed for the solution to converge.

This can be seen in the initiation of buckling in the ((16,0),(25,0)) DWNT as compared to that in the (25,0) SWNT. The SWNT begins to buckle at an angle of twist/length of 0.046 while the DWNT with only the outer tube loaded (slip condition) buckles at a much higher angle of twist/length of 0.109. Thus van der Waals forces between the two walls delay the buckling of the outer tube. However, when both walls are simultaneously twisted (fully constrained case) then the angle of twist/length at the onset of buckling drops back down to 0.047. In each case, there is a gradual transition into the buckled shape, as opposed to the snap-through behavior found for buckling under axial loads. As should become transparent from the deformed shapes plotted in Figure 3.9 the buckled shape of the outer wall of the DWNT is similar to that of its inner SWNT.

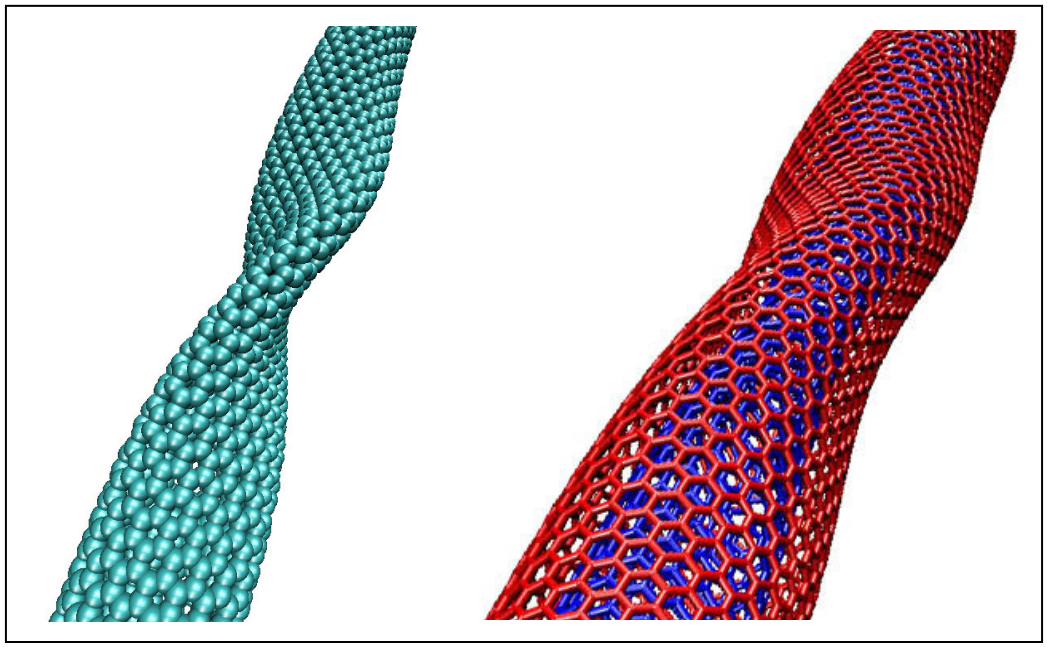

Figure 3.9. Buckled shapes of (16,0) SWNT, and ((16,0),(25,0)) DWNT under torsional loads.

3.3.3 Expression for van der Waals forces

Batra and Sears[23] simulated the radial expansion/contraction of a wall of a DWNT, and computed the intermolecular energy, W, due to van der Waals forces only as a function of the distance, *s,* between the two walls; their results are summarized in Figure 3.10. Equation (2) describes the least squares fit to the data:

$$W = 2\pi L \frac{K(b(s+r_i)+1)}{b^2(r_o^2 - r_i^2)} \exp[-b(s-c)], \tag{3.2}$$

where 2.6 Å < s < 3.5 Å, K = 9.5 ×10^{-22} J/ Å^3, b = 5.3 1/ Å, c = 3.52 Å, and r_0 and r_i are, respectively, the radii of the outer and the inner tubes. The radial force versus s relation is found by differentiating Eq. (2) with respect to s from which pressure is computed. The resulting pressure (van der Waals force/area) versus the radial strain relation is depicted in Figure 3.11, and is used to deduce the axial force versus the axial displacement relation for a truss element in the following section.

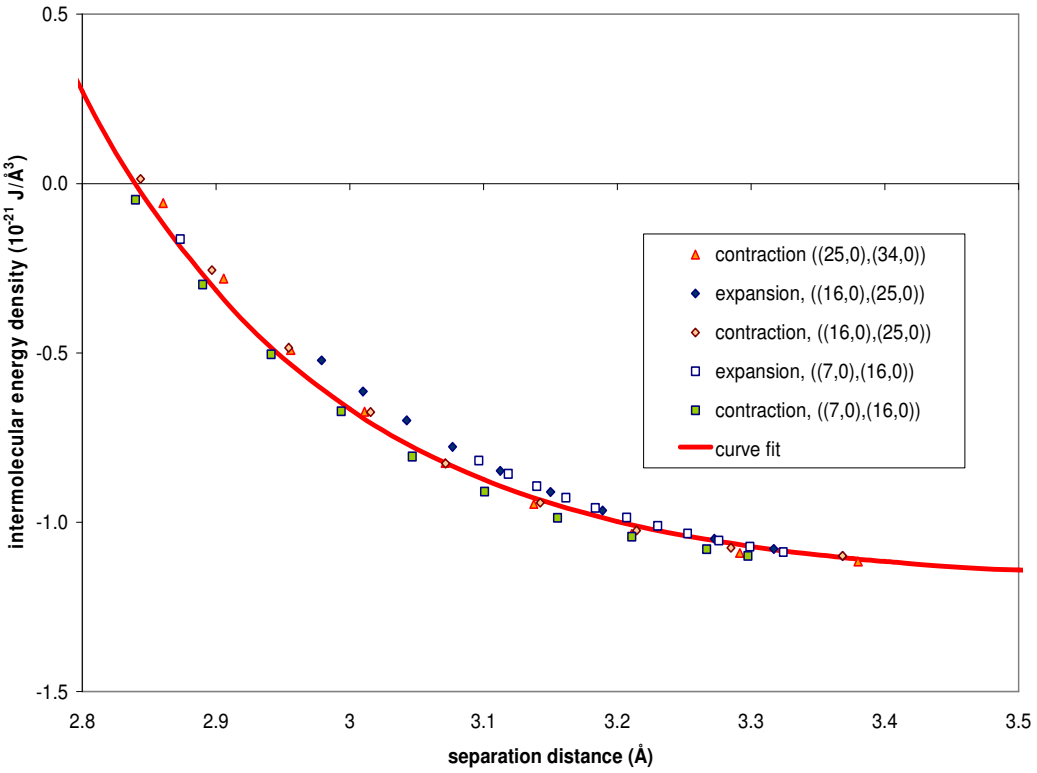

Figure 3.10. Strain energy due to van der Waals force vs. distance between two adjacent walls of a DWNT; results for three DWNTs lie on the same curve.

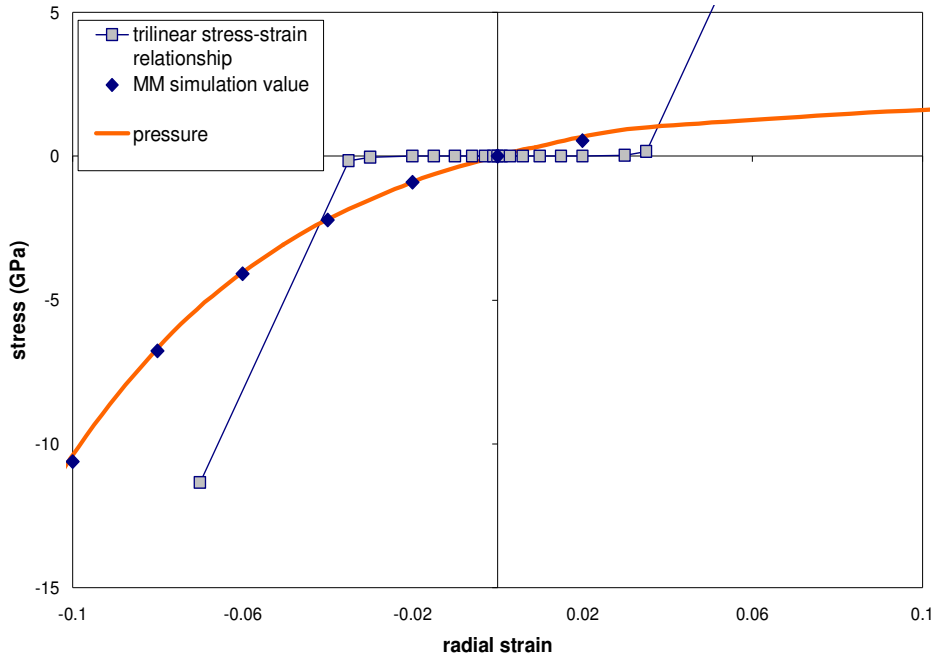

Figure 3.11. Radial pressure vs. radial strain derived from MM simulations of radial expansion/contraction of a wall of a nanotube

3.4 Equivalent continuum structure

As mentioned above, we found in a previous study[4] that the response of an initially stress-free continuum cylindrical tube made of a homogeneous and isotropic linear elastic material with mean radius of the continuum tube = radius of the SWNT, t = 1.34 Å, E = 2.54 TPa, G = 0.96 TPa, is equivalent to that of a SWNT for axial, torsional and bending deformations. Furthermore, for large values of length/diameter, the axial strain at the onset of buckling due to axial loads predicted by the Euler buckling theory applied to the equivalent continuum structure equaled that obtained through MM simulations of deformations of the SWNT. Values of E, G and t were found to be independent of the helicity and the radius of the SWNT. It has been shown here that, prior to the onset of buckling, the response of a DWNT to axial and torsional deformations is essentially the same as that of a SWNT. Since SWNT MM simulation results may be used to predict deformations of a MWNT it is reasonable to propose that a continuum structure equivalent to a MWNT be comprised of concentric cylindrical tubes each of thickness 1.34 Å and having E = 2.54 TPa, G = 0.96 TPa. The adjacent concentric tubes are

interconnected by an appropriate number of truss elements aligned radially and with the area of cross-section varying affinely to ensure that equal and opposite forces are exerted on the adjacent walls of a MWNT. The end faces of a truss are connected to the cylindrical tube through rollers that can slide freely in the circumferential direction. The equivalent continuum model is shown schematically in Figure 3.12. The axial modulus of a truss element is taken to vary with the axial strain according to the pressure vs. radial strain curve depicted in Figure 3.11. The area of cross-section, A_t, of a truss element depends upon the number of trusses employed and Young's modulus, E_t , of the material of truss elements. Thus A_t E_t multiplied with the number of truss elements should equal the surface area of a wall multiplied by the van der Waals pressure acting on it. One can reduce the number of truss elements by increasing the value of E_t.

Since the length of each truss element will not change during constrained deformations of a MWNT in which both walls are deformed simultaneously by the same amount, it will not exert any radial force on either of the two walls. The length of a truss element will not change when either one of the two walls of a DWNT is twisted with no loads applied to the other wall. However, when one of the two walls of a DWNT is compressed axially then the length of a truss element will change and it will exert a radial force on the two walls it connects.

In the analysis of deformations of a DWNT by the finite element method, the number of truss elements will equal the number of nodes on each wall of the cylindrical tube.

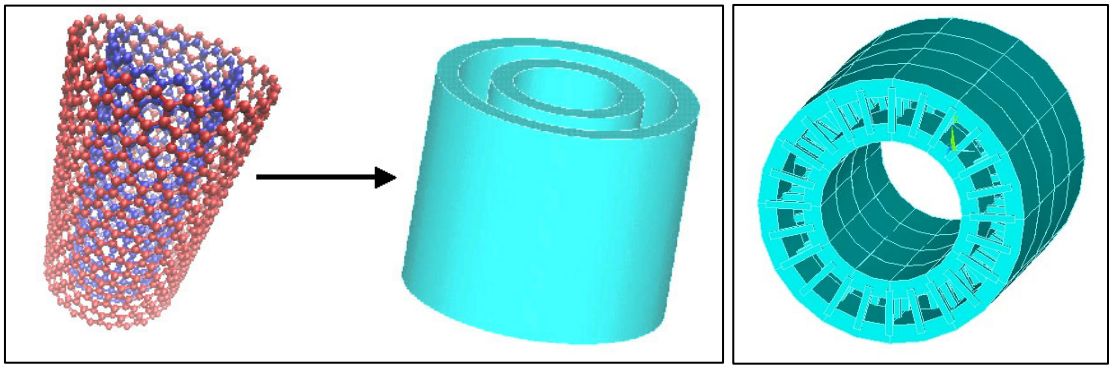

Figure 3.12. Left: a continuum structure equivalent to a DWNT; Right: a cross-section showing trusses connecting the two concentric tubes to account for van der Walls force.

While van der Waals forces are long range forces, their magnitude diminishes rapidly when the distance between two atoms exceeds the ideal wall separation distance of 3.4 Å, which can be seen from the expression for U_{VdW} in Eq. (1). Thus, while truss elements will not capture the longer range, weaker and dispersed forces from many atoms, they effectively account for the shorter range forces which are much higher in magnitude

During columnar buckling, the length of truss elements will not change much and thus they will not exert much radial force on either wall to which they are connected. This will leave the wall separation distance essentially unchanged as has been observed in TEM images of bent nanotubes[24, 25].

3.5 Validation of the Continuum Model

3.5.1 Bending Deformations

Bending deformations of three DWNT cantilever beams of various helicities and radii have been analyzed with the MM3 potential. For a prescribed deflection of the free end, the Euler beam theory is used to estimate the deformed positions of atoms. The null displacement boundary conditions at the clamped edge are enforced by fixing positions of atoms of the outer wall that are ~5 Å from one end of the tube. The prescribed deflection at the other end is achieved by displacing three adjacent atoms ~10 Å from the free end of the tube to minimize the wall indentation effects. With boundary conditions applied to atoms on the outer wall only, van der Waals forces act on atoms of the inner wall. These boundary conditions mimic an experimental set-up where only the outer wall is loaded. For each prescribed deflection, axial positions of all atoms, including those with assigned lateral displacements (or deflections), were perturbed to find the minimum energy configuration of the bent tube.

As can be seen from the deformed configurations plotted in Figure 3.13, for the three DWNTs of varying wall structures, the wall separation distance remained constant at points away from the atoms where displacements were prescribed. Thus truss elements can be ignored during bending deformations of a MWNT. The deformed shape of the DWNT found by MM simulations agrees well with that given by the Euler beam theory.

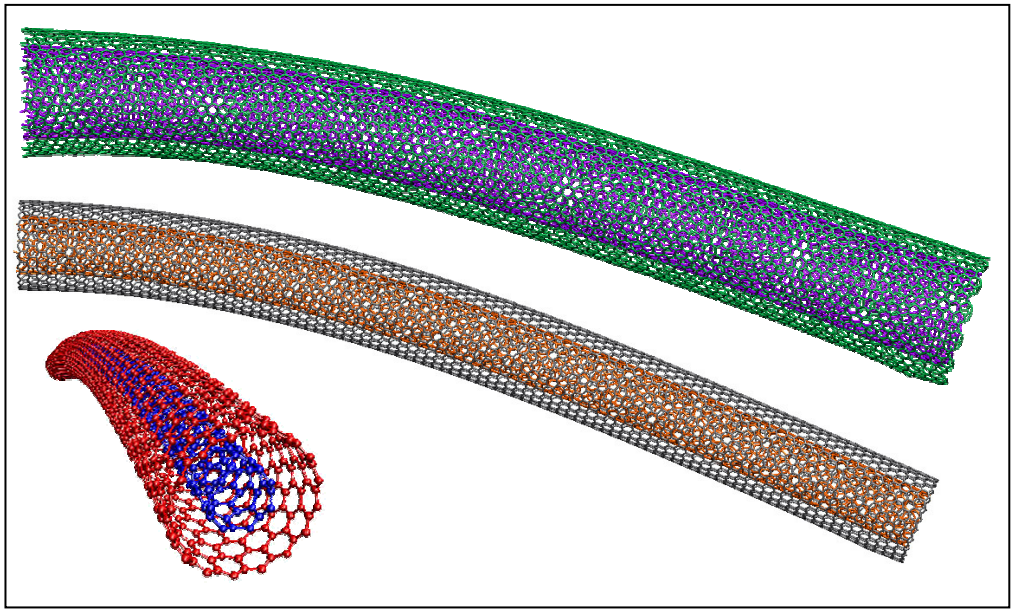

Figure 3.13. Deformed configurations of three cantilever DWNTs loaded by a point load at the free end.

Strain energies computed from the Euler beam theory applied to the equivalent continuum structure and from the MM simulations on the DWNT and the SWNTs are plotted in Figure 3.14. The close agreement between the strain energies computed by the two methods validates the proposed equivalent continuum structure.

We have plotted in Figure 3.15 strain energies of bending computed by using the Euler beam theory and two other continuum structures; one of these, referred to as CS2 proposed by Yakobson et al.[26], has a wall thickness of 0.66 Å which equals the thickness of the pi-bond. The other continuum structure, referred to as CS3, commonly used has outer diameter equal to that of the outer wall of the tube and a wall thickness of 6.8 Å. The presently proposed continuum structure is called CS1. Values of E for these three continuum structures were adjusted so that EA is the same for them; here A equals the area of cross-section of the continuum structure. Several trends can be deduced from the plots. First, the structures CS3 require higher strain energy of bending due to their higher area moment of inertia. Second, the difference among results from structures CS1, CS2 and CS3 diminishes as the radius of the DWNT increases because the radius to thickness ratio becomes higher. Lastly, except for the continuum structure CS3 corresponding to the smallest diameter tube, the three equivalent continuum structures give results close to those obtained from MM simulations.

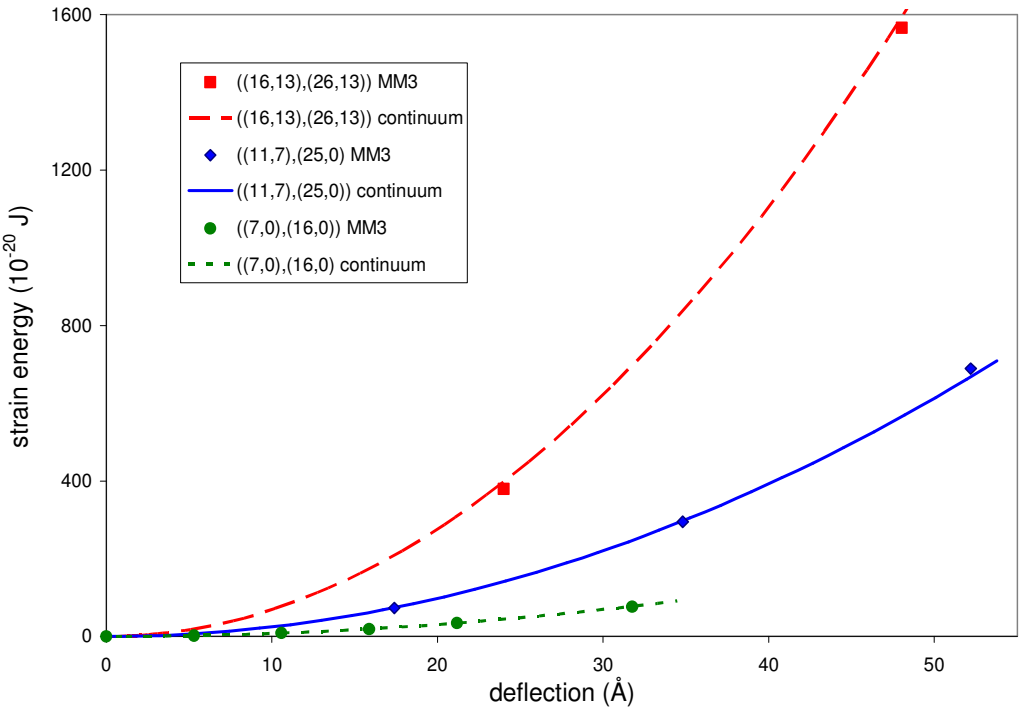

Figure 3.14. Strain energies of cantilever DWNTs with a point load at the unclamped end computed by MM simulations and the Euler beam theory using the equivalent continuum model.

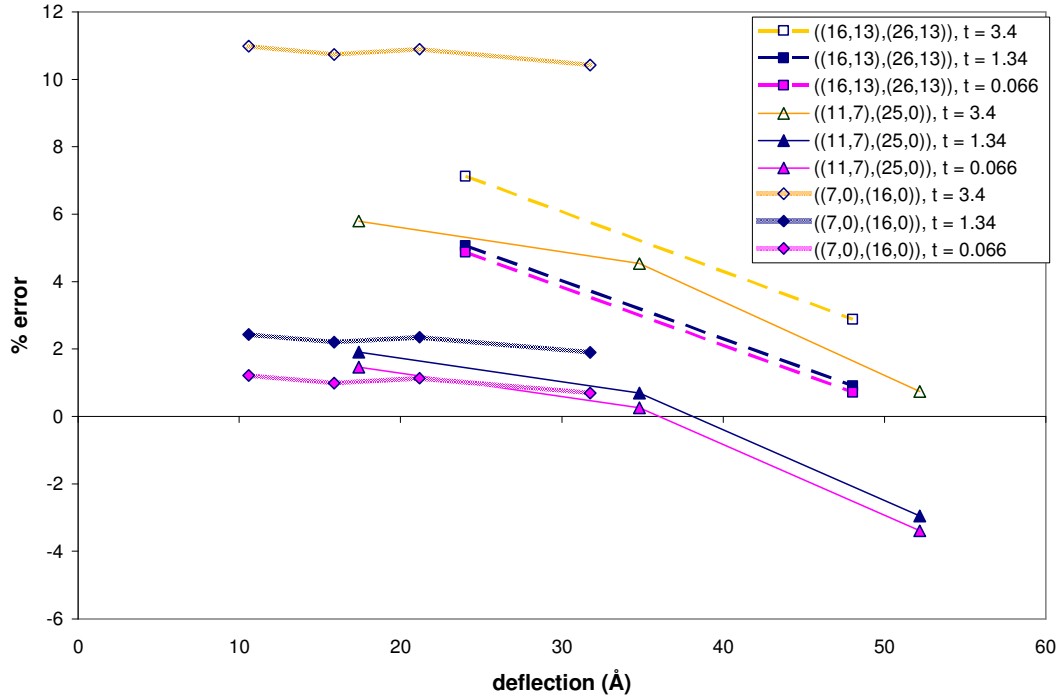

Figure 3.15. Variation with the tip deflection of the percentage error in the strain energy computed by using the Euler beam theory for continuum structures equivalent to the three DWNTs. The three colors correspond to different values of the tube thickness.

3.5.2 Buckling Deformations

In Figure 3.16 we have plotted the axial strain at the onset of buckling vs. the tube length obtained through MM simulations for two DWNTs and one constituent SWNT, and also that computed by using the Euler buckling theory and FEA for continuum structures equivalent to the SWNTs and the DWNTs proposed herein. Some example buckling shapes for FE models of DWNTs are presented in Figure 3.17. A carbon nanotube was assumed to buckle when the strain energy of deformation for an incremental additional axial compression suddenly dropped; e.g. see results plotted in Figure 3.4. It is evident that for tubes with length/outer diameter exceeding about 10, results from the Euler buckling theory applied to continuum structures match very well with those from the MM simulations thereby validating the proposed equivalent continuum structure. Sears and Batra[23] have shown that truss elements play a noticeable role when analyzing buckling deformations of DWNTs with small values of length/outer diameter.

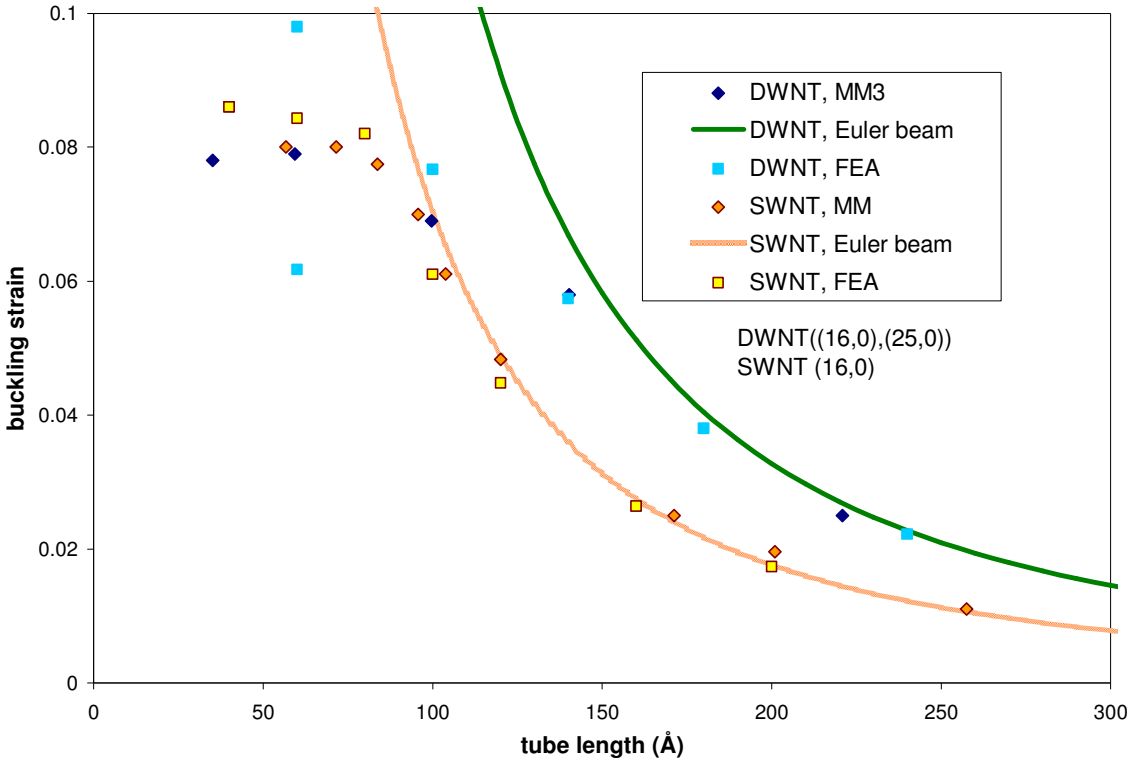

Figure 3.16. Variation with the tube length of the axial strain at buckling for two differently structures DWNTs, their constituent SWNTs, and that predicted by the Euler buckling theory and FEA by using the equivalent continuum model.

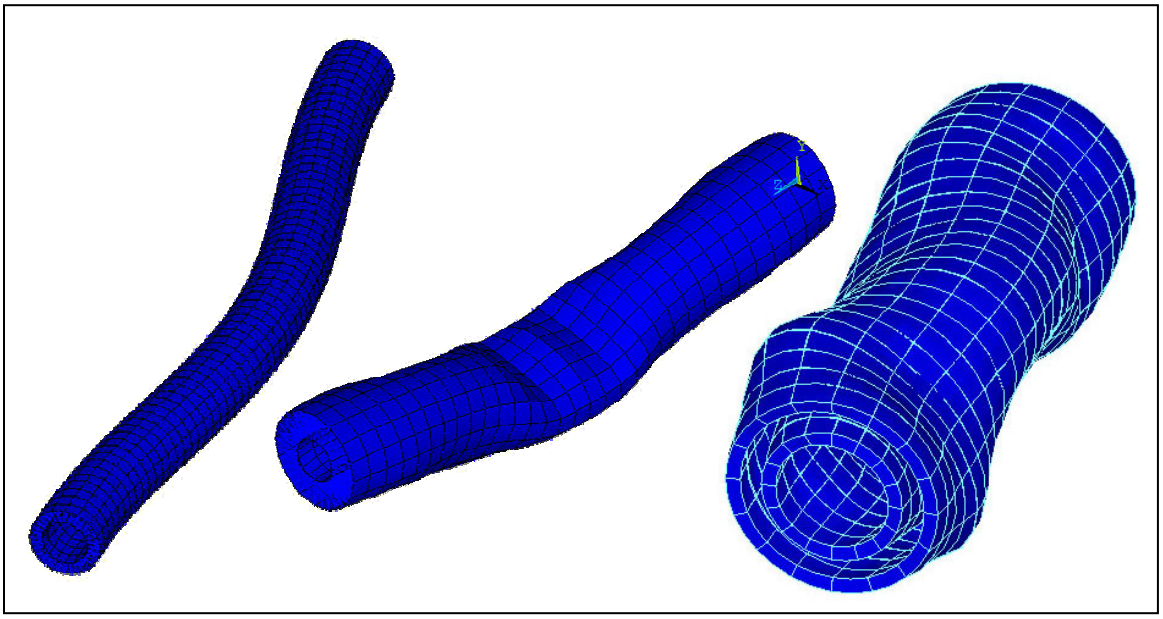

Figure 3.17. Examples of various FEA DWNT buckled shapes; (left): column buckling, (middle): column buckling with crimping, (right): shell wall buckling

3.6 Conclusions

We have used results of MM simulations on DWNTs and a TWNT under various loads to answer several questions about the similarities/differences of their responses with those of the constituent SWNTs. Based on these results we have proposed a continuum structure whose response to mechanical deformations is the same as that obtained with MM simulations on the DWNT. The proposed equivalent continuum structure is simple and may be used with various engineering analytical techniques such as Euler beam theory or finite element analysis depending on the type of response being studied and level of sophistication desired. It has been validated by comparing predictions from it for bending and columnar buckling deformations with those derived from the MM simulations.

An advantage of having an equivalent continuum structure is that it can be used to compute effective properties of composites comprised of polymers reinforced with MWNTs. Also, an equivalent continuum structures is inherently used to interpret results of experiments on carbon nanotubes and deduce values of material parameters.

Answers to questions posited in Section 1 are as follows: (i) walls of a MWNT slide freely over each other in both axial and torsional loading of only one wall; (ii) except for

buckling deformations, results for a MWNT may be obtained within 3% accuracy by adding those for the constituent SWNTs subjected to the same traction or displacement boundary conditions; (iii) the wall separation distance is of primary importance when finding energetically favorable MWNT configurations while differences in their helical angles play a minor role in the relative axial translation of walls; (iv) for bending deformations, the choice of an equivalent continuum structure was found not to be highly important as long as they had the same axial stiffness and the radius to wall thickness ratio was large. During torsional loading with the same angle of twist/length applied to each wall of a DWNT, the buckled shape of the DWNT resembles that of its constituent inner SWNT.

Acknowledgements

This work was partially supported by the ONR grants N00014-98-1-0300 and N00014-06-1-0567 to Virginia Polytechnic Institute and State University (VPI&SU) with Dr. Y. D. S. Rajapakse as the program manager. Opinions expressed in the paper are those of the authors and neither of the funding agency nor of VPI&SU.

References

1 S. Iijima, Nature **354**, 56 (1991).
2 J. Cunnings and A. Zettl, Science **289**, 602 (2000).
3 B. A. Galanov, S. B. Galanov, and Y. Gogotsi, Journal of Nanoparticle Research **4** (2002).
4 A. Sears and R. C. Batra, Physical Review B **69** (2004).
5 D. Qian, G. J. Wagner, W. K. Liu, et al., Applied Mechanics Review **55**, 495 (2002).
6 C. Schonenberger, A. Bachtold, C. Strunk, et al., Applied Physics A **69** (1999).
7 M.-F. Yu, O. Lourie, M. J. Dyer, et al., Science **287**, 637 (2000).
8 M.-F. Yu, B. I. Yakobson, and R. S. Ruoff, Journal of Physical Chemistry B. **104**, 8764 (2000).
9 M. M. J. Treacy, T. W. Ebbesen, and J. M. Gibson, Nature **381**, 678 (1996).
10 J.-P. Salvetat, J.-M. Bonard, N. H. Thomson, et al., Applied Physics A **69**, 255 (1999).
11 E. W. Wong, P. E. Sheehan, and C. M. Lieber, Science **277**, 1971 (1997).
12 O. Lourie and H. Wagner, Journal of Materials Research **13**, 1471 (1998).
13 C. Li and T.-W. Chou, International Journal of Solids and Structures **40**, 2487 (2003).
14 C. Q. Ru, Journal of Applied Physics **89**, 3426 (2001).

15 K. M. Liew, C. H. Wong, X. Q. He, et al., Physical Review B **69**, 115429 (2004).
16 A. Pantano, D. M. Parks, and M. C. Boyce, Journal of the Mechanics and Physics of Solids **52**, 789 (2004).
17 T. Belytschko, S. P. Xiao, G. C. Schatz, et al., Physical Review B **66** (2002).
18 M. Arroyo and T. Belytschko, International Journal for Numerical Methods in Engineering **59**, 419 (2003).
19 P. Zhang, Y. Huang, P. H. Geubelle, et al., International Journal of Solids and Structures **39**, 3893 (2002).
20 N. L. Allinger, Y. H. Yuh, and J.-H. Lii, Journal of the American Chemical Society **111**, 8551 (1989).
21 J. W. Ponder, (Washington University in St. Loius, St. Louis, 2000).
22 C. T. White, D. H. Robertson, and J. W. Mintmire, Physical Review B **47**, 5485 (1992).
23 A. Sears and R. C. Batra, Physical Review B **73** (2006).
24 C. Bower, R. Rosen, L. Jin, et al., Applied Physics Letters **74**, 3317 (1999).
25 O. Lourie, D. M. Cox, and H. D. Wagner, Physical Review Letters **81**, 1638 (1998).
26 B. I. Yakobson, C. J. Brabec, and J. Bernholc, Physical Review Letters **76**, 2511 (1996).